Chemical Engineering Journal 244 (2014) 364–371

Contents lists available at ScienceDirect

Chemical Engineering Journal

journal homepage: www.elsevier.com/locate/cej

Toward predicting the mercury removal by chlorine on the ZnO surface

Lixia Ling [a,b], Senpeng Zhao [a], Peide Han [b], Baojun Wang [c,*], Riguang Zhang [c], Maohong Fan [d]

[a] Research Institute of Special Chemicals, Taiyuan University of Technology, Taiyuan 030024, Shanxi, PR China
[b] College of Materials Science and Engineering, Taiyuan University of Technology, Taiyuan 030024, Shanxi, PR China
[c] Key Laboratory of Coal Science and Technology, Taiyuan University of Technology, Ministry of Education and Shanxi Province, Taiyuan 030024, Shanxi, PR China
[d] Department of Chemical and Petroleum Engineering, University of Wyoming, Laramie, WY 82071, USA

HIGHLIGHTS

- $HgCl_2$ is directly formed by the adsorbed Cl and Hg^0 on the ZnO surface and not via HgCl intermediate.
- The dissociated H atoms on the ZnO surface inhibit the formation of $HgCl_2$.
- Cl_2 rather than HCl is responsible for the oxidation of Hg^0 on the ZnO surface.
- $HgCl_2$ is easy to be formed via the E–R and L–H mechanisms on the ZnO surface.

GRAPHICAL ABSTRACT

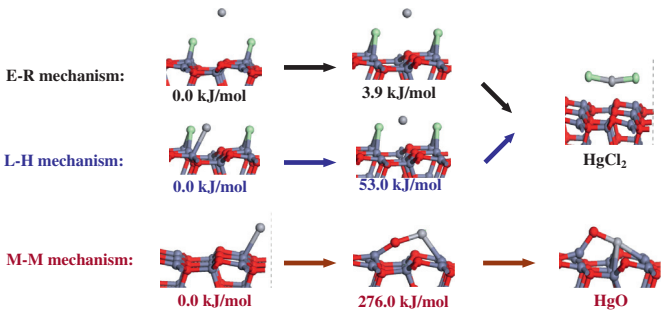

ARTICLE INFO

Article history:
Received 10 November 2013
Received in revised form 24 January 2014
Accepted 25 January 2014
Available online 2 February 2014

Keywords:
Hg^0 removal
Coal
Flue gas
Oxidation mechanism
Density functional theory

ABSTRACT

The density functional theory with the generalized gradient approximation has been used to determine the binding mechanism of Cl_2, HCl and Hg species on the ZnO($10\bar{1}0$) surface, and the Hg^0 oxidation mechanism by Cl_2 (or HCl) on the ZnO surface. Cl_2 and HCl are dissociatively adsorbed on the surface, and Cl atom bonds to two adjacent Zn atoms. Binding energy of Hg^0 is showing a physisorption mechanism, while $HgCl_2$ is strongly adsorbed on the surface in the molecularly mode, which indicates that the oxidation of Hg^0 is necessary for its removal from flue gas. HgCl is not an indispensable intermediate during the Hg^0 oxidation to form $HgCl_2$. Three Hg^0 oxidation mechanisms have been investigated, and the $HgCl_2$ is easy to be formed via both the Eley–Rideal and Langmuir–Hinshelwood mechanisms, while Mars–Maessen mechanism is unfavorable since high activation energy is needed for Hg^0 reacting with the lattice oxygen of ZnO. The adsorbed H atoms by HCl dissociation inhibit the formation of $HgCl_2$, and Cl_2 is the primary species being responsible for the Hg^0 oxidation on the ZnO surface.

1. Introduction

The emission of mercury (Hg) in coal has attracted a growing attention due to its large impact on environment and mankind health [1–3]. Mercury is vaporized from the coal and mainly exists in the elemental mercury (Hg^0) form, which is the most difficult species to be removed from the coal-derived flue gas because of its exceedingly high volatility, low water solubility, and relative chemical inertness [4,5]. An effective method being considered to control the Hg^0 emission in the flue gas is oxidizing Hg^0 with oxidants like Cl_2 or HCl over a catalyst, followed by the removal of the resulting oxidized mercury [6–9]. $HgCl_2$ is generally thought to be the main oxides in the coal-derived flue gas, which is slightly less volatile and better water–soluble than Hg^0 [10].

Cl_2 is an effective oxidant for the conversion of Hg^0 to $HgCl_2$ [11]. Laudal et al. [12] have injected Cl_2 into their simulated flue

* Corresponding author. Address: No. 79 Yingze West Street, Taiyuan 030024, PR China. Tel.: +86 351 6018239; fax: +86 351 6041237.
E-mail address: wangbaojun@tyut.edu.cn (B. Wang).

http://dx.doi.org/10.1016/j.cej.2014.01.080
1385-8947/

gas and concluded that Cl_2 instead of HCl, is responsible for Hg^0 oxidation. Conversely, it is observed that there is a direct relation between the concentration of HCl in a simulated flue gas and the extent of mercury oxidation [13,14], and a good correlation between the fraction of mercury in the oxidized state and the mercury removal from the flue gas [15]. The effects of HCl on the Hg^0 removal from coal derived fuel gases over CeO_2/TiO_2 and $V_2O_5(WO_3)/TiO_2$ have been investigated. The results show that HCl exhibits a promotional effect on Hg^0 oxidation over CeTi catalyst [16] and the Hg^0 oxidation rate is enhanced by increasing HCl concentration [17]. CuO also exhibits significant catalytic activity for the Hg^0 oxidation in the presence of HCl [18]. However, the presence of HCl inhibits the Hg^0 removal rate by Fe_2O_3 [19,20], which suggests that the effect of HCl on Hg removal varies from one catalyst to another. Therefore it is urgent and necessary for Hg removal to seek for an efficient material, which requires two important aspects: (1) extensive evaluation of currently used and new catalysts, and (2) a more comprehensive understanding of the reaction mechanism [21]. Recently, the activated carbon prepared by chemical activation using zinc chloride ($ZnCl_2$) has showed significant mercury adsorption capability because Hg^0 is oxidized by the oxidative elements on the surface of activated carbon [22], while it prepared by steam activation do not adsorb Hg^0 in nitrogen environment [23,24]. In this process, Cl atoms which are created by $ZnCl_2$ impregnation, are involved by probably forming various complexes, e.g. $[HgCl]^+$, $[HgCl_2]$ and $[HgCl_4]^{2-}$ [25].

Nowadays, experimental information is not always sufficient and computational chemistry methodologies have been used to further insight into the material properties, mechanisms of adsorption and oxidation [26,27]. The oxidation mechanism and kinetics of Hg^0 by chlorine [28] and bromine [29] were investigated using quantum chemistry, and several important reaction parameters were obtained. The binding mechanisms of mercury species, including Hg^0, HgCl and $HgCl_2$, on the α-Fe_2O_3 (001) and V_2O_5(001) surfaces were also investigated by using the density functional theory (DFT) [30,31] and the oxidation pathway for Hg^0 by HCl was presented. On the CaO(100) and CaO(001) surfaces, HgCl and $HgCl_2$ were chemisorbed while Hg^0 was physisorbed [32,33]. Negreira et al. [34] investigated the oxidation of Hg^0 by HCl on the vanadia dimer supported on the TiO_2(001) surface. It could draw a conclusion that the oxidation follows a Langmuir–Hinshelwood mechanism due to the stronger HCl and HgCl interaction with the surface, and then $HgCl_2$ was formed. In addition, our latest work [35] using theoretical method has shown that Hg^0 is physically adsorbed on the ZnO($1\,0\,\bar{1}\,0$) surface, which implies the poor removal rate of Hg^0. However, the adsorbed active S by H_2S dissociation easily captures Hg^0 to form stable HgS, contributing to Hg^0 removal. Soon afterwards, a latest related research by Zhou et al. [36] verified our prediction. The nano-ZnO sorbents have been synthesized by a homogeneous precipitation method, and it can be concluded that Hg removal rate is about 11% by nano-ZnO sorbent, while only 6% by ZnO sorbent. Furthermore, the effect of H_2S on the average Hg^0 removal rate in 2 h are shown that the Hg^0 removal rate gradually increases with the H_2S concentration increased, even the rate reaches 95.6% when 0.08% H_2S is introduced to the gas flow. The above facts indicate that the theoretical study not only can illustrate the experimental results, but also can predict and evaluate the properties of materials. In addition, a number of metal oxides like CuO, Fe_2O_3, CaO, V_2O_5, MnO_2, CeO_2 and ZnO, have similar properties in desulfurization [37,38]. And the former six materials can convert Hg^0 to $HgCl_2$ in the presence of Cl_2 or HCl, contributing to the mercury removal [39,40]. However, The Hg^0 removal rate in the presence of Cl_2 (or HCl) by the ZnO sorbent remains unknown. And Hg oxidation on the ZnO surface prefers to proceed via a Langmuir–Hinshelwood (L–H) [41] or an Eley–Rideal (E–R) [42] or a Mars–Maessen (M–M) mechanism [43], is not clear. In the L–H mechanism, both Hg and Cl_2 (or HCl) are adsorbed on the ZnO($1\,0\,\bar{1}\,0$) surface, and subsequently, $HgCl_2$ is formed [44]. In contrast, in the E–R mechanism, Cl_2 (or HCl) is adsorbed on the surface, then a Hg atom from the gas phase directly attacks the adsorbed Cl species leading to the formation of $HgCl_2$ [45]. The M–M mechanism is the oxidation of Hg^0 by a lattice oxidant to form HgO [46].

The goal of our theoretical study is to provide fundamental insight into Hg^0 oxidation by Cl_2 (or HCl) on the ZnO surface, including the binding mechanisms of Cl_2 (or HCl) and Hg species on the ZnO surface, and the reaction mechanism between Cl_2 (or HCl) and Hg^0. In the Hg^0 oxidation process, whether HgCl is the indispensable and important intermediate, and whether Cl_2 or HCl is the primary species and responsible for this oxidation, will be understood. In addition, the influence of dissociated H atoms by HCl on the formation of $HgCl_2$ will also be explained.

2. Computational model and method

2.1. Computational model

A reasonable computational model is very important to describe, explain, and even predict an experimental fact. ZnO($1\,0\,\bar{1}\,0$) surface was selected to characterize the oxidation mechanism of Hg^0 by Cl_2 (or HCl) as its electronic stability and being main surface of ZnO [47–51]. Fig. 1 displays the configurations of the top view and side view of ZnO($1\,0\,\bar{1}\,0$) surface. Six chemically different types of adsorption sites on the ZnO($1\,0\,\bar{1}\,0$) surface were considered, including "Zn–top", "O-top", "short Zn–O bridge", "long Zn–O bridge", "Zn–Zn bridge" and "O–O bridge" sites, corresponding to I, II, III, IV, V and VI, respectively.

The calculations on the $p(3 \times 2)$ surfaces were performed by using slab models of eight layers. A lot of theoretical studies have shown that the 8-layer slab model adequately represents the ZnO($1\,0\,\bar{1}\,0$) surface [52–54]. The bottom two layers of the slab were kept fixed at their bulk-like positions, while the remaining atoms in the top six layers and the adsorbed molecules or atoms were allowed to relax. The vacuum layer of 10 Å along the *z*-direction was assumed to avoid the interactions between periodic slabs of atomic layers.

2.2. Computational method

Density functional theory (DFT) is a quantum mechanical modeling method used in physics and chemistry to investigate the electronic structure of materials, thereby determine their properties [55]. The generalized gradient approximation (GGA) with Perdew–Wang 1991 function [56,57] and a doubled-numerical-quality basis set with polarization functions (DNP) [58] were used for all the calculations. The inner electrons of Zn atoms and Hg atoms were kept frozen and replaced by an effective core potential (ECP) [59], and other atoms in this study were treated with an all-electron basis set. The calculations were carried out by using the Brillouin zone sampled with a $3 \times 2 \times 1$ Monkhorst–Pack mesh *k*-points grid, and the real space cutoff radius was maintained as 4.4 Å. Meanwhile, transition state (TS) search was performed at the same theoretical level with the complete linear synchronous transit and quadratic synchronous transit (LST/QST) method [60], starting from reactant and product, the LST method performs a singly interpolation to a maximum energy, and the QST method alternates searches for an energy maximum with constrained minimizations in order to refine the transition states to a high degree [61,62]. In addition, TS confirmation was done on every transition state structure to demonstrate that it leaded to the desired reactant and product using the nudged elastic band

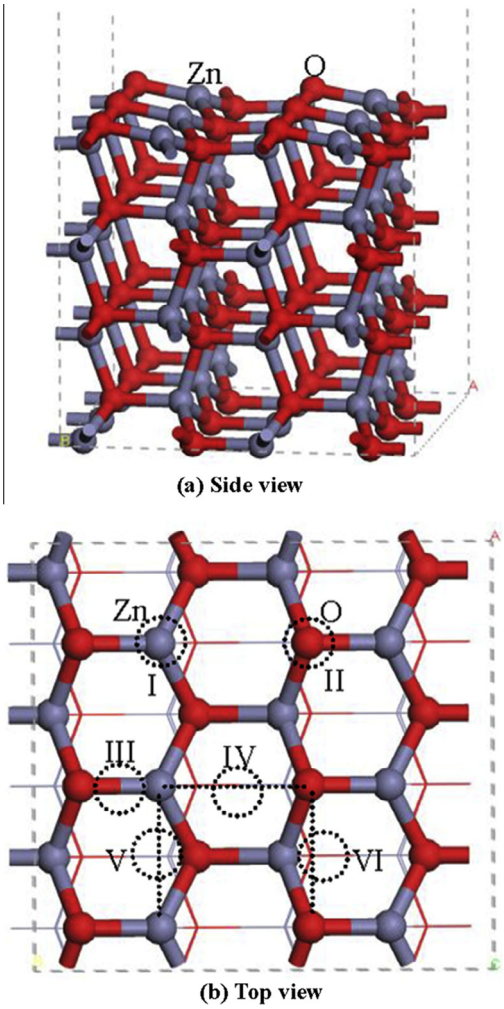

Fig. 1. The slab model of the ZnO(1 0 $\bar{1}$ 0)–(3 × 2). (a) Side view of the ZnO(1 0 $\bar{1}$ 0) surface; (b) top view of the ZnO(1 0 $\bar{1}$ 0) surface. I, II, III, IV, V and VI correspond to active sites for "Zn–top", "O–top", "short Zn–O bridge", "long Zn–O bridge", "Zn–Zn bridge", and "O–O bridge" sites, respectively. The dot line represents the supercell used in this study.

(NEB) method [63]. All calculations were carried out with the Dmol^3 program available in Materials studio 5.5 package [64,65]. The reason for selecting the method and parameters are provided in the Supplementary information. The adsorption energies, E_{ads}, are calculated as follows:

$$E_{ads} = E_{tot}(ads) + E_{tot}(slab) - E_{tot}(ads/slab) \quad (1)$$

where E_{tot}(ads) is the total energy of the free adsorbate in the gas phase, E_{tot}(slab) is the total energy of the bare slab, and E_{tot}(ads/slab) is the total energy for the slab with adsorbate in its equilibrium geometry.

3. Results and discussion

3.1. Hg^0 adsorption on the ZnO(1 0 $\bar{1}$ 0) surface

The most stable adsorption structure of Hg^0 on the ZnO(1 0 $\bar{1}$ 0) surface is that Hg atom is bound to the surface Zn atom with the adsorption energy of 27.0 kJ·mol^{-1}, which is similar to the cases on the α-Fe_2O_3(0 0 1) [30] and CuO(1 1 0) [66] surfaces, in which Hg atom interacts with the metal atom. However, on the CaO(1 0 0) [32] and V_2O_5(0 0 1) surfaces [31], the mercury–oxygen interactions are more favorable. Mulliken population analysis and the partial density of states (PDOS) are calculated to analyze the interaction between adsorbed Hg and the ZnO(1 0 $\bar{1}$ 0) surface. Little electrons of 0.120*e* transferring from Hg atom to the surface implies that Hg atom is weakly bound to the surface Zn atom. The PDOS in Fig. 2 shows that the sharp peak of *d* state is not changed after Hg adsorbing, and only *s* and *p* states slightly broaden, which indicates Hg^0 is physically adsorbed on the ZnO(1 0 $\bar{1}$ 0) surface [35], and the recent experiment has also authenticated it [36]. The similar result has also been investigated on the vanadia dimer supported on the TiO_2(0 0 1) surface [34], CaO(1 0 0) [32] and CaO(0 0 1) surfaces [33,67,68], the adsorption energies are 3.8, 12.3 and 21.5–31.4 kJ·mol^{-1}, respectively. However, Hg has a strong interaction with the noble metal Pd comparing with ZnO, as a result of a significant overlap between the *s*- and *p*-states of Pd and the *d*-states of Hg [69].

3.2. Cl_2 adsorption on the ZnO(1 0 $\bar{1}$ 0) surface

Three different adsorption structures are obtained when Cl_2 are placed on the ZnO(1 0 $\bar{1}$ 0) surface with different original models, which are shown in Fig. 3, and the adsorption energies are shown in Table 1. Cl_2(a) and Cl_2(b) are the molecular adsorption of Cl_2, the bond lengths of Cl–Cl are 2.166 and 2.178 Å, and the adsorption energies are 50.4 and 61.2 kJ·mol^{-1}, respectively. In Cl_2(c), Cl_2 is dissociatively adsorbed on the surface, and two Cl atoms are at two adjacent Zn–Zn bridge sites. The adsorption energy is 130.0 kJ·mol^{-1}, which shows that Cl atom prefers to adsorb at the Zn–Zn bridge site.

3.3. HCl adsorption on the ZnO(1 0 $\bar{1}$ 0) surface

For the asymmetric HCl molecule, two adsorption modes on the ZnO(1 0 $\bar{1}$ 0) surface are considered: one is an end-on mode involving HCl being perpendicular to the surface via the Cl or H atom approaching to the surface, and the other is a side-on mode involving HCl being parallel to the surface. Fifteen possible initial adsorption configurations are presented in Fig. S1 (Supplementary information). Five different adsorption structures are obtained, as shown in Fig. 4. The perpendicular orientation of HCl is illustrated, and it has been found that H adsorbs at the O atom site with a weak interaction, while Cl desorbs. Another possible configuration for the perpendicular adsorption HCl on the ZnO(1 0 $\bar{1}$ 0) surface is with the Cl atom located closer to the surface O. However, this results in HCl being far away from the surface with a weak interaction of 6.4 kJ·mol^{-1}. Calculated adsorption energies show that the

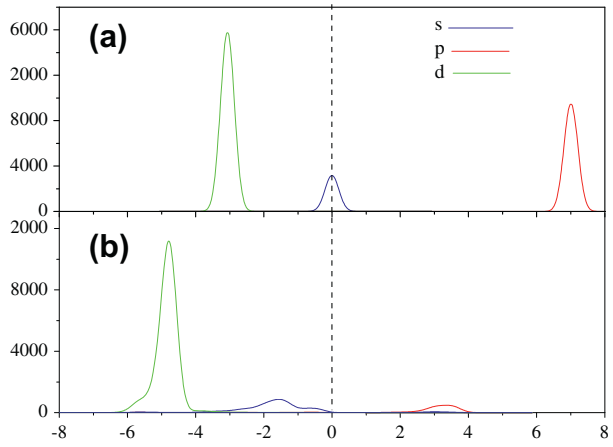

Fig. 2. PDOS analysis of Hg atom before and after adsorption on the ZnO(1 0 $\bar{1}$ 0) surface. (a) the free Hg atom and (b) the adsorbed Hg atom.

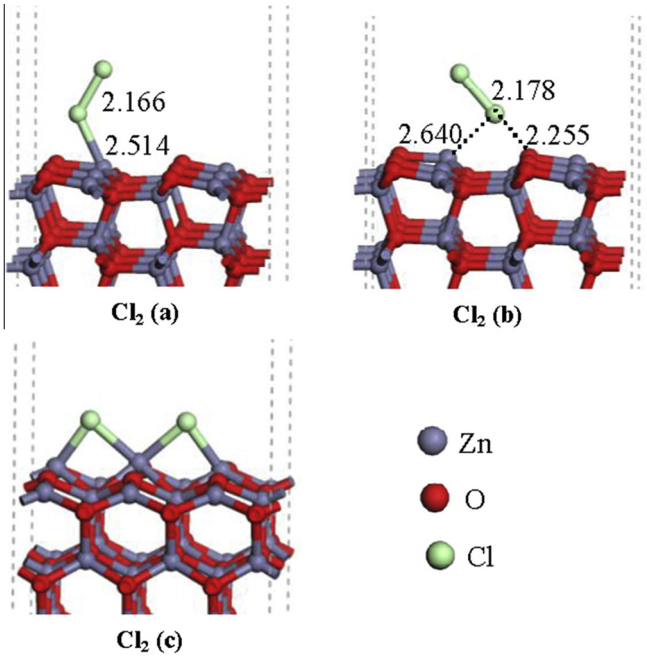

Fig. 3. Optimized adsorption configurations of Cl_2 on the ZnO(10$\bar{1}$0) surface. The bond lengths are given in Å.

Table 1
The adsorption energies of Cl_2, HCl and $HgCl_2$ on the ZnO(10$\bar{1}$0) surface (kJ·mol^{-1}).

Species	E_{ads}	Species	E_{ads}	Species	E_{ads}	Species	E_{ads}
Cl_2(a)	50.4	HCl(a)	176.8	HgCl(a)	84.5	$HgCl_2$(a)	13.0
Cl_2(b)	61.2	HCl(b)	174.7	HgCl(b)	82.3	$HgCl_2$(b)	10.4
Cl_2(c)	130.0	HCl(c)	60.0	HgCl(c)	72.6	$HgCl_2$(c)	40.2
		HCl(d)	6.4	HgCl(d)	71.5	$HgCl_2$(d)	22.4
		HCl(e)	183.4	HgCl(e)	128.7	$HgCl_2$(e)	57.9
				HgCl(f)	128.6	$HgCl_2$(f)	116.8
				HgCl(g)	125.8	$HgCl_2$(g)	115.7
				HgCl(h)	98.5		
				HgCl(i)	132.6		
				HgCl(j)	137.5		
				HgCl(k)	138.6		

parallel orientations of HCl are favorable, in which Cl is bonded to the surface Zn with a single bond or bridge bond. As a consequence, HCl competes with Hg^0 for the active Zn sites. This is consistent with the adsorption of Hg^0 and HCl on the vanadia-based catalyst when HCl adsorbs onto the catalyst surface in a pure N_2 environment and competes with the weakly adsorbed Hg^0 for the active sites [70].

3.4. HgCl adsorption on the ZnO(10$\bar{1}$0) surface

Cl atom prefers to adsorb on the surface Zn atom in the bridge bond mode, and Hg atom binding with the surface Zn atom is also the most stable configuration. The two atoms in HgCl are competitive for the active Zn site, thus the adsorption modes are needed to be studied.

Similar to the case of HCl, all the fifteen possible initial adsorption modes of HgCl on the ZnO(10$\bar{1}$0) surface are investigated, and eleven optimized equilibrium configurations are obtained, as shown in Fig. 5. There are only four adsorption configurations of HgCl with the molecular modes, and the others are the dissociative modes. The adsorption energies of HgCl show that the dissociative adsorption structures are favorable compared with the molecular structures, which is in line with the adsorption of HgCl on the

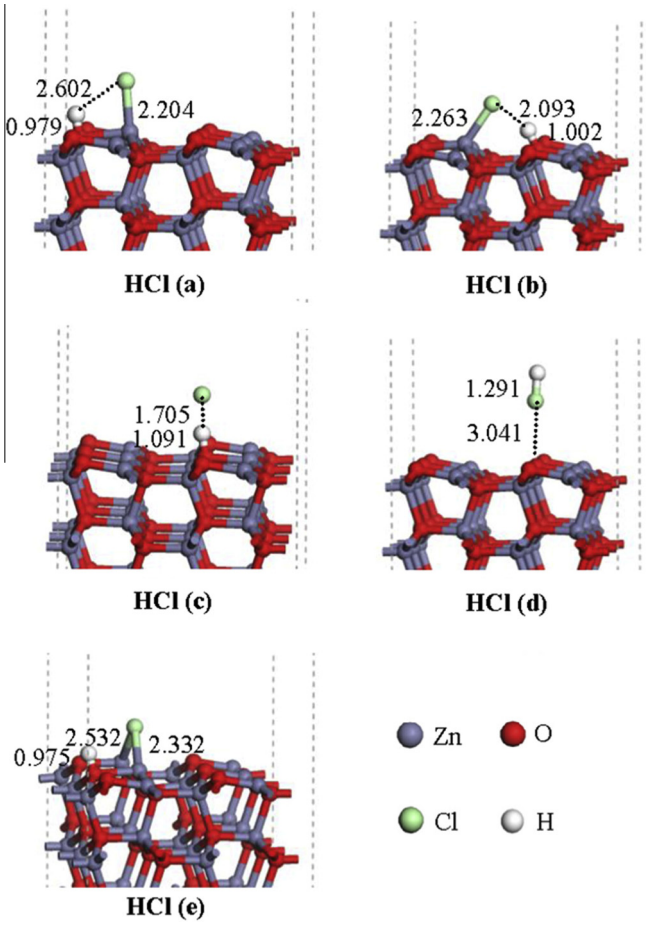

Fig. 4. Optimized adsorption configurations of HCl on the ZnO(10$\bar{1}$0) surface.

CaO(100) surface, and the adsorption energies of the stable configurations on these two surfaces are 138.6 and 100.3 kJ·mol^{-1} [32], respectively. Only trace amount of HgCl existing in molecular mode explains why the concentration of HgCl cannot be measured directly with experiments [71,72]. On the α-Fe_2O_3(001) surface [30], HgCl also primarily exists in dissociative mode. It implies that HgCl is not a stable intermediate during the Hg^0 oxidation by Cl_2 or HCl on the ZnO(10$\bar{1}$0) and α-Fe_2O_3(001) surfaces. However, HgCl is formed following an E–R mechanism via gas phase Hg interacting with adsorbed HCl on vanadia–titania catalyst, and then reacts with HCl leading to the formation of $HgCl_2$ [34]. In addition, HgCl molecularly adsorbing on the V_2O_5(001) surface at different sites has been investigated [31]. Thus, unlike the case on the ZnO(10$\bar{1}$0) surface, HgCl is an important intermediate for the Hg^0 oxidation over the vanadia catalyst.

3.5. $HgCl_2$ adsorption on the ZnO(10$\bar{1}$0) surface

$HgCl_2$ is initially placed at different adsorption sites in perpendicular and parallel orientations. The seven calculated and optimal configurations of $HgCl_2$ are shown in Fig. 6, and their adsorption energies are displayed in Table 1. For the perpendicular cases, they have little adsorption energies, implying weak interaction between the perpendicular structures and the surface. For the parallel cases, the most stable structures are $HgCl_2$(f) and $HgCl_2$(g). The molecule $HgCl_2$ is linear, and the between Hg and Cl decreased to 167.332° and 167.088° on the surface. Hg prefers to the O top site in $HgCl_2$(f) and to the O–O bridge site in $HgCl_2$(g), while the two Cl atoms are stable at the Zn top site and the Zn–Zn bridge sites. The similar

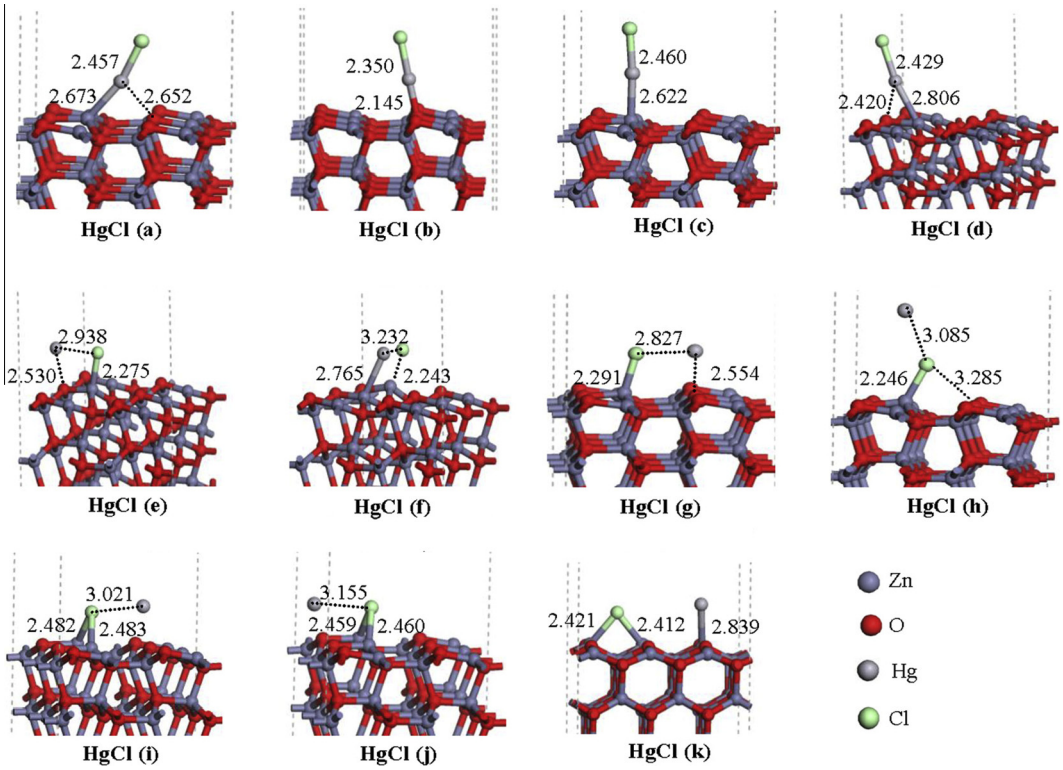

Fig. 5. The optimized equilibrium configurations of HgCl adsorbed on the ZnO(10$\bar{1}$0) surface.

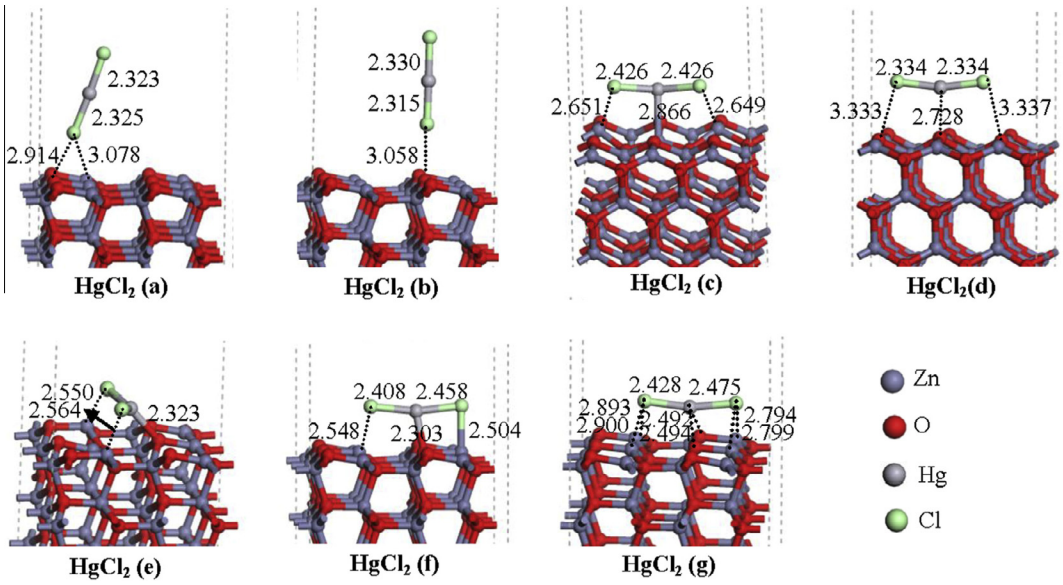

Fig. 6. The optimized equilibrium configurations of $HgCl_2$ adsorbed on the ZnO(10$\bar{1}$0) surface.

conclusion has been obtained by other researcher's report on the CaO(100) surface [32], and an experimental study has reported that $HgCl_2$ can be captured in parallel on the CaO surface with the attractions of both acidic (Ca^{2+}) and basic (O^{2-}) sites [73]. Meanwhile, it can be found that the adsorption energy of $HgCl_2$ on the ZnO(10$\bar{1}$0) surface is little higher than that on the CaO(100) surface with 90.0 kJ·mol^{-1} [32] and little lower than that on the CaO(001) surface with 147.6 kJ·mol^{-1} [68]. However, the current results do not agree with the results of Guo et al. [30], and the most stable configuration of $HgCl_2$ on the α-Fe_2O_3(001) surface is a dissociative adsorption.

3.6. Hg^0 oxidation on the ZnO surface

Wilcox et al. [26] have explored the current state of knowledge associated with the homogeneous and heterogeneous reaction pathways, and the adsorption mechanism on various materials are discussed. In addition, several critical reviews [21,26,39] believed that a degree of predictability in the performance of the catalyst will be needed, and a detailed mechanism and kinetic are needed to develop to explain and predict the Hg^0 oxidation removal. Thus, three possible mechanisms associated with Hg^0 oxidation on the ZnO surface are investigated. The most favorable

adsorption configurations of Cl_2, HCl, Hg^0 and $HgCl_2$ determine the initial configurations of the reactants and products in the Hg^0 oxidation pathways. The potential energy diagram for the Hg^0 oxidation pathway by Cl_2 on the ZnO(1 0 $\bar{1}$ 0) surface is obtained and presented in Fig. 7. The reaction pathway for the direct formation of $HgCl_2$ is investigated through the reaction between the adsorbed Cl and adsorbed Hg (or Hg in gas) due to the low concentration of HgCl, which is in agreement with the finding of Senior et al. [71,72].

When the E–R mechanism is proposed to explain the reaction, two Cl atoms adsorbed at two nonadjacent Zn–Zn bridge sites according to the formed $HgCl_2$(g), and Hg atom in gas is far away from the adsorbed Cl atom [R(E–R) in Fig. 7]. Then, Hg atom approaches to the surface Cl atoms, and a little activation barrier of 3.9 kJ·mol^{-1} is needed to overcome at TS(E–R) leading to the formation of $HgCl_2$(g), implying that the formation of $HgCl_2$ is easy. L–H mechanism is also applied to investigate the Hg^0 oxidation. During the study, two Cl atoms resulting from the dissociation of Cl_2 and Hg atom are separately adsorbed at their stable sites on the ZnO(1 0 $\bar{1}$ 0) surface, the adsorbed species react and form $HgCl_2$ via TS(L–H) with the activation energy of 53.0 kJ·mol^{-1}. The relatively low energy barrier makes the $HgCl_2$ formation moderately easy. The L–H mechanism has also been proposed to explain the mercury oxidation on the vanadia-based catalyst in experiment, where the active Cl generated from adsorbed HCl reacts with adjacent Hg^0 leading to the formation of $HgCl_2$ [70]. In these two reaction processes, $HgCl_2$ is directly formed via the dissociated Cl atom and Hg without HgCl intermediate. However, a different oxidation process of Hg^0 has been obtained on the Au(1 1 1) surface, in which Hg oxidation prefers a pathway of HgCl serving as an intermediate for the eventual formation of $HgCl_2$, rather than a pathway directly oxidizing Hg to $HgCl_2$ [74].

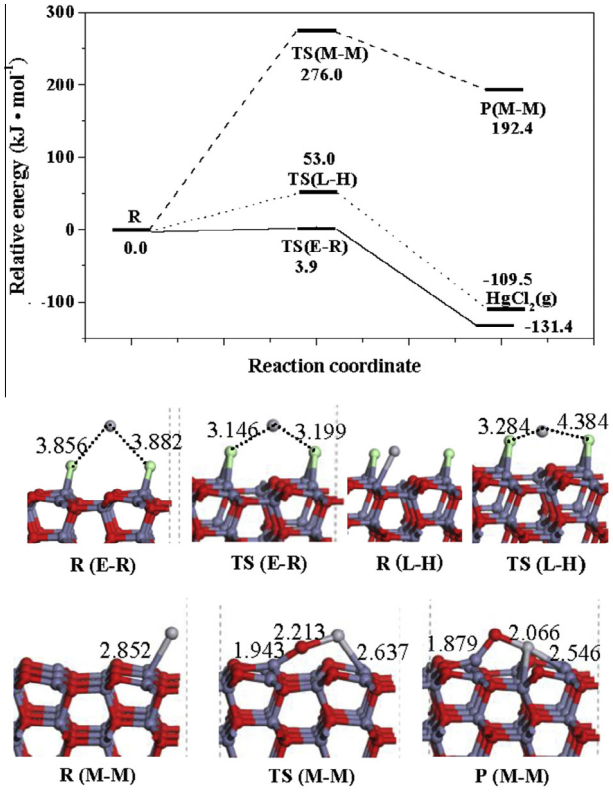

Fig. 7. Potential energy diagram for the oxidation pathway of Hg^0 by Cl_2 on the ZnO surface.

In addition, the M–M mechanism of the Hg^0 reacting with a lattice oxygen on the ZnO surface has also been investigated. The oxygen-deficient ZnO surface is formed followed by the oxidation of Hg^0, and HgO adsorbs on the oxygen defect surface. Two adsorption configurations are obtained, one is that O atom in HgO fills the oxygen defect, and Hg adsorbs at the Zn site, which is the same as the structure of Hg atom adsorbing on the perfect ZnO(1 0 $\bar{1}$ 0) surface; the other is that HgO adsorbs at the deficient site with an adsorption energy of 339.5 kJ·mol^{-1}, which is as the oxidation product of Hg^0, named P(M–M) (see Fig. 7). An activation barrier of 276.0 kJ·mol^{-1} is needed to overcome to form HgO, indicating that the M–M mechanism is less favorable than the L–H and E–R mechanisms for the Hg^0 oxidation.

The oxidation of Hg^0 by HCl is also investigated in this research. An examination of the energy diagram clearly indicates that the adsorptions of HCl and Hg are the exothermal processes, which is shown in Fig. S2. A HCl and a Hg atom adsorb on the surface with a reaction energy of −212.6 kJ·mol^{-1}, and the adsorption mode of HCl is the same as that of single HCl without Hg adsorbing. The adsorption energy of HCl is 185.6 kJ·mol^{-1} when it is co-adsorbed with Hg on the ZnO(1 0 $\bar{1}$ 0) surface, which is a little difference with only 2.2 kJ·mol^{-1} compared with the adsorption of single HCl. And then another HCl adsorbs on the surface with a reaction energy of −200.0 kJ·mol^{-1}. In the adsorption process, the HCl molecule dissociatively adsorbs on the surface, and Cl atoms bonds to the surface Zn atoms to form $ZnOCl_2$ species. The similar structure $VOCl_2$ resulting from reaction between gaseous HCl and V_2O_5 has also been reported by others [75]. This suggests that HCl participates in Hg^0 oxidation in a form of adsorbed species and Cl bounds with Zn atom.

Then, the formation of $HgCl_2$ is studied. However, it is unfortunately that the $HgCl_2$ is not formed on the surface when the adsorbed H atoms are present, showing that the presence of H is disadvantageous to the Hg^0 oxidation. The similar result has been obtained with experimental study of Hg^0 removal by Fe_2O_3 in the presence of HCl [19,20]. However, HCl is an effective flue gas component for Hg^0 oxidation over CeTi catalyst, which can be adsorbed and reacted with the catalyst to form active oxychloride. And then, the active surface species react with adsorbed Hg^0 leading to $HgCl_2$ via HgCl intermediate with the L–H mechanism [16]. On the Au(1 1 1) surface, the H atom due to HCl dissociation consumes the electron charge of the gold atoms, and lowers the strength of interaction between the gold atoms and the reaction intermediates. Eventually HCl enhances the Hg oxidation reaction by lowering the activation energy for the formation of HgCl and $HgCl_2$ [74]. The situation on the ZnO(1 0 $\bar{1}$ 0) surface is different. The charge of 0.132*e* transfers from H atoms to the surface during dissociatively adsorption of HCl on the surface, thereby strengthens the interaction between the adsorbed Cl atom and surface, which ultimately inhibits the Hg^0 oxidation. Future work will focus on exploring the experimental conditions, where different flue gas components like HCl and Cl_2 will be considered, which could validate the predicted results.

4. Conclusions

The density functional theory and periodic model have been used to study the binding mechanisms of Hg^0, Cl_2, HCl, HgCl and $HgCl_2$ molecules on the ZnO surface. It is determined that Hg^0 is preferably adsorbed on the ZnO(1 0 $\bar{1}$ 0) surface at the Zn atom with the physisorption. Cl_2 and HCl are mainly dissociatively adsorbed on the ZnO(1 0 $\bar{1}$ 0) surface, and Cl atom prefers to adsorb at the Zn–Zn bridge site. HgCl mainly exists in dissociative mode and is not stable intermediate. $HgCl_2$ as the oxidative product of Hg^0 is adsorbed on the ZnO(1 0 $\bar{1}$ 0) surface in molecular mode.

Both Eley–Rideal and Langmuir–Hinshelwood mechanisms are viable for the ZnO-catalyzed Hg^0 oxidation, $HgCl_2$ is directly formed through the reaction of the adsorbed Cl with adsorbed Hg or Hg in gas, and the activation energies are 3.9 and 53.0 $kJ \cdot mol^{-1}$, respectively. The Mars–Maessen mechanism is unfavorable for this reaction due to a high activation barrier. The dissociated H atoms on the surface inhibit the formation of $HgCl_2$, and Cl_2 is the primary species being responsible for the Hg^0 oxidation on the ZnO surface.

Acknowledgments

This work was supported by the National Natural Science Foundation of China (Grant Nos. 20976115, 21276171, 21276003), the National Younger Natural Science Foundation of China (Grant No. 21103120), China Postdoctoral Science Foundation (Grant No. 2012M520608), Wyoming Clean Coal Program and the State Key Laboratory of Fine Chemicals (KF1205).

Appendix A. Supplementary material

Supplementary data associated with this article can be found, in the online version, at http://dx.doi.org/10.1016/j.cej.2014.01.080.

References

[1] R.N. Sliger, J.C. Kramlich, N.M. Marinov, Towards the development of a chemical kinetic model for the homogeneous oxidation of mercury by chlorine species, Fuel Process Technol. 65–66 (2000) 423–438.
[2] H.Q. Yang, Z.H. Xu, M.H. Fan, A.E. Bland, R.R. Judkins, Adsorbents for capturing mercury in coal-fired boiler flue gas, J. Hazard. Mater. 146 (2007) 1–11.
[3] R.A. Monterrozo, M.H. Fan, M. Asce, M.D. Argyle, Adsorption of mercury with modified thief carbons, J. Environ. Eng. 138 (2012) 386–391.
[4] S.J. Yang, Y.F. Guo, N.Q. Yan, D.Q. Wu, H.P. He, Z. Qu, C. Yang, Q. Zhou, J.P. Jia, Nanosized cation-deficient Fe–Ti spinel: a novel magnetic sorbent for elemental mercury capture from flue gas, Appl. Mater. Interfaces 3 (2) (2011) 209–217.
[5] S. Kellie, Y. Cao, Y.F. Duan, L.C. Li, P. Chu, A. Mehta, R. Carty, J.T. Riley, W.P. Pan, Factors affecting mercury speciation in a 100-MW coal-fired boiler with low-NOx burners, Energy Fuels 19 (3) (2005) 800–806.
[6] M.A. Uddin, T. Yamada, R. Ochiai, E. Sasaoka, S.J. Wu, Role of SO2 for elemental mercury removal from coal combustion flue gas by activated carbon, Energy Fuels 22 (4) (2008) 2284–2289.
[7] B. Hall, O. Lindqvist, E. Ljungström, Mercury chemistry in simulated flue gases related to waste incineration conditions, Environ. Sci. Technol. 24 (1) (1990) 108–111.
[8] B. Hall, P. Schager, O. Lindqvist, Chemical reactions of mercury in combustion flue gases, Water Air Soil Pollut. 56 (1) (1991) 3–14.
[9] N.C. Widmer, J.A. Cole, W.R. Seeker, J.A. Gaspar, Practical limitation of mercury speciation in simulated municipal waste incinerator flue gas, Combust. Sci. Technol. 134 (1–6) (1998) 315–326.
[10] R. Meij, L.H.J. Vredenbregt, H. te Winkel, The fate and behavior of mercury in coal-fired power plants, J. Air Waste Manage. Assoc. 52 (8) (2002) 912–917.
[11] H. Agarwal, H.G. Stenger, S. Wu, Z. Fan, Effects of H_2O, SO_2, and NO on homogeneous Hg oxidation by Cl_2, Energy Fuels 20 (3) (2006) 1068–1075.
[12] D.L. Laudal, T.D. Brown, B.R. Nott, Effects of flue gas constituents on mercury speciation, Fuel Process. Technol. 65–66 (2000) 157–165.
[13] C. Lee, R. Srivastava, S. Ghorishi, T. Hastings, F. Stevens, Investigation of selective catalytic reduction impact on mercury speciation under simulated NOx emission control conditions, J. Air Waste Manage. Assoc. 54 (12) (2004) 1560–1566.
[14] S. Eswaran, H. Stenger, Understanding mercury conversion in selective catalytic reduction (SCR) catalysts, Energy Fuels 19 (6) (2005) 2328–2334.
[15] R. Meij, The fate of mercury in coal-fired power plants and the influence of wet flue-gas desulphurization, Water Air Soil Pollut. 56 (1) (1991) 21–33.
[16] H.L. Li, C.Y. Wu, Y. Li, J.Y. Zhang, CeO_2–TiO_2 catalysts for catalytic oxidation of elemental mercury in low-rank coal combustion flue gas, Environ. Sci. Technol. 45 (2011) 7394–7400.
[17] H. Kamata, S. Ueno, T. Naito, A. Yukimura, Mercury oxidation over the $V_2O_5(WO_3)/TiO_2$ commercial SCR catalyst, Ind. Eng. Chem. Res. 47 (21) (2008) 8136–8141.
[18] S.B. Ghorishi, C.W. Lee, W.S. Jozewicz, J.D. Kilgroe, Effects of fly ash transition metal content and flue gas HCl/SO_2 ratio on mercury speciation in waste combustion, Environ. Eng. Sci. 22 (2) (2005) 221–231.
[19] S.J. Wu, M. Ozaki, M.A. Uddin, E. Sasaoka, Development of iron-based sorbents for Hg^0 removal from coal derived fuel gas: effect of hydrogen chloride, Fuel 87 (4–5) (2008) 467–474.
[20] M. Ozaki, M.A. Uddin, E. Sasaoka, S.J. Wu, Temperature programmed decomposition desorption of the mercury species over spent iron-based sorbents for mercury removal from coal derived fuel gas, Fuel 87 (17–18) (2008) 3610–3615.
[21] A.A. Presto, E.J. Granite, Survey of catalysts for oxidation of mercury in flue gas, Environ. Sci. Technol. 40 (18) (2006) 5601–5609.
[22] P.Y. Zhang, H.C. Zeng, L. Zhang, Experiments on mercury adsorption by activated carbon, Elec. Power Sci. Eng. 2 (2004) 1–3.
[23] C.X. Hu, J.S. Zhou, S. He, Z.Y. Luo, K.F. Cen, Effect of chemical activation of an activated carbon using zinc chloride on elemental mercury adsorption, Fuel Process. Technol. 90 (6) (2009) 812–817.
[24] P. Fang, C.P. Cen, D.S. Chen, Z.X. Tang, X.Y. Li, Hg vapor adsorption of sludge carbon adsorbents made by $ZnCl_2$ chemical activation in simulated flue gas, Chin. J. Environ. Eng. 3 (2) (2009) 311–316.
[25] H.C. Zeng, F. Jin, J. Guo, Removal of elemental mercury from coal combustion flue gas by chloride-impregnated activated carbon, Fuel 83 (1) (2004) 143–146.
[26] J. Wilcox, E. Rupp, S.C. Ying, D-H. Lim, A.S. Negreira, A. Kirchofer, F. Feng, K. Lee, Mercury adsorption and oxidation in coal combustion and gasification process, Int. J. Coal Geol. 90–91 (2012) 4–20.
[27] R.G. Zhang, L.Z. Song, B.J. Wang, Z. Li, A density functional theory investigation on the mechanism and kinetics of dimethyl carbonate formation on Cu_2O catalyst, J. Comp. Chem. 33 (11) (2012) 1101–1110.
[28] J. Wilcox, A kinetic investigation of high-temperature mercury oxidation by chlorine, J. Phys. Chem. A 113 (24) (2009) 6633–6639.
[29] J.A. Tossell, Calculation of the energetics for oxidation of gas-phase elemental Hg by Br and BrO, J. Phys. Chem. A 107 (39) (2003) 7804–7808.
[30] P. Guo, X. Guo, C.G. Zheng, Computational insights into interactions between Hg species and α-$Fe_2O_3(001)$, Fuel 90 (5) (2011) 1840–1846.
[31] J. Liu, M.F. He, C.G. Zheng, M. Chang, Density functional theory study of mercury adsorption on $V_2O_5(001)$ surface with implications for oxidation, Proc. Combust. Inst. 33 (2) (2011) 2771–2777.
[32] E. Sasmaz, J. Wilcox, Mercury species and SO_2 adsorption on CaO(100), J. Phys. Chem. C 112 (42) (2008) 16484–16490.
[33] X. Guo, P.F. Zhao, C.G. Zheng, Theoretical study of different speciation of mercury adsorption on CaO(001) surface, Proc. Combust. Inst. 32 (2009) 2693–2699.
[34] A.S. Negreira, J. Wilcox, DFT study of Hg oxidation across Vanadia–Titania SCR catalyst under flue gas conditions, J. Phys. Chem. C 117 (4) (2013) 1761–1772.
[35] L.X. Ling, P.D. Han, B.J. Wang, R.G. Zhang, Theoretical prediction of simultaneous removal efficiency of ZnO for H_2S and Hg^0 in coal gas, Chem. Eng. J. 231 (2013) 388–396.
[36] J.S. Zhou, P. Qi, W.H. Hou, S.L. You, X. Gao, Z.Y. Luo, Elemental mercury removal from syngas by nano-ZnO sorbent, J. Fuel Chem. Technol. 41 (11) (2013) 1371–1377.
[37] D. Vamvuka, C. Arvanitidis, D. Zachariadis, Flue gas desulfurization at high temperature: a review, Environ. Eng. Sci. 21 (4) (2004) 525–547.
[38] S. Cheah, D.L. Carpenter, K.A. Magrini-Bair, Review of mid- to high-temperature sulfur sorbents for desulfurization of biomass- and coal-derived syngas, Energy Fuels 23 (2009) 5291–5307.
[39] Y.S. Gao, Z. Zhang, J.W. Wu, L.H. Duan, A. Umar, L.Y. Sun, Z.H. Guo, Q. Wang, A critical review on the heterogeneous catalytic oxidation of elemental mercury in flue gases, Environ. Sci. Technol. 47 (2013) 10813–10823.
[40] B.-A. Dranga, L. Lazar, H. Koeser, Oxidation catalysts for elemental mercury in flue gases-a review, Catalysts 2 (2012) 139–170.
[41] R.J. Baxter, P. Hu, Insight into why the Langmuir–Hinshelwood mechanism is generally preferred, J. Chem. Phys. 116 (11) (2002) 4379–4381.
[42] C. Bürgel, N.M. Reilly, G.E. Johnson, R. Mitrić, M.L. Kimble, A.W. Castleman Jr., V. Bonačić-Koutecký, Influence of charge state on the mechanism of CO oxidation on gold clusters, J. Am. Chem. Soc. 130 (2008) 1694–1698.
[43] E.J. Granite, H.W. Pennline, R.A. Hargis, Novel sorbents for mercury removal from flue gas, Ind. Eng. Chem. Res. 39 (4) (2000) 1020–1029.
[44] Y. Eom, S.H. Jeon, T.A. Ngo, J. Kin, T.G. Lee, Heterogeneous mercury reaction on a selective catalytic reduction (SCR) catalyst, Cata. Lett. 121 (2008) 219–225.
[45] S. Niksa, N. Fujiwara, A predictive mechanism for mercury oxidation on selective catalytic reduction catalysts under coal-derived flue gas, J. Air Waster Manage. Assoc. 55 (2005) 1866–1875.
[46] W. Lee, G.-N. Bae, Removal of elemental mercury (Hg(0)) by nanosized V_2O_5/TiO_2 catalysts, Environ. Sci. Technol. 43 (2009) 1522–1527.
[47] A. Wander, N.M. Harrison, An ab initio study of ZnO($10\bar{1}0$), Surf. Sci. 457 (1–2) (2000) L342–L346.
[48] B. Meyer, H. Rabaa, D. Marx, Water adsorption on ZnO($10\bar{1}0$): from single molecules to partially dissociated monolayers, Phys. Chem. Chem. Phys. 8 (13) (2006) 1513–1520.
[49] J.B.L. Martins, J. Andrés, E. Longo, C.A. Taft, A theoretical study of (101)–(0) and (0001) ZnO surfaces: molecular cluster model, basis set and effective core potential dependence, J. Mol. Struct.–THEOCHEM 330 (1–3) (1995) 301–306.
[50] N.L. Marana, V.M. Longo, E. Longo, J.B.L. Martins, J.R. Sambrano, Electronic and structural properties of the (101(−)0) and (112(−)0) ZnO surfaces, J. Phys. Chem. A 112 (38) (2008) 8958–8963.
[51] C.B. Duke, R.J. Meyer, A. Paton, P. Mark, Calculation of low-energy-electron-diffraction intensities from ZnO($10\bar{1}0$). II. Influence of calculational procedure, model potential, and second-layer structural distortions, Phys. Rev. B 18 (8) (1978) 4225–4240.
[52] H.Q. Hu, Z.T. Lv, S.X. Cui, G.Q. Zhang, Theoretical study of ZnO($10\bar{1}0$) and M/ZnO($10\bar{1}0$) (M=Cu, Ag and Au) surfaces with DFT approach, Chem. Phys. Lett. 510 (1–3) (2011) 99–103.

[53] J. Hu, W.P. Guo, X.R. Shi, B.R. Li, J.G. Wang, Copper deposition and growth over ZnO nonpolar $(10\bar{1}0)$and $(11\bar{2}0)$ surfaces: a density functional theory study, J. Phys. Chem. C 113 (17) (2009) 7227–7235.
[54] B. Meyer, D. Marx, Density-functional study of the structure and stability of ZnO surfaces, Phys. Rev. B 67 (3) (2003). 035403-1-11.
[55] W. Koch, M.C. Holthausen, A Chemist's Guide to Density Functional Theory, second ed., Wiley-VCH Verlag GmbH, 2001.
[56] J.P. Perdew, K. Burke, M. Ernzerhof, Generalized gradient approximation made simple, Phys. Rev. Lett. 77 (18) (1996) 3865–3868.
[57] J.P. Perdew, K. Burke, Y. Wang, Generalized gradient approximation for the exchange-correlation hole of a many-electron system, Phys. Rev. B: Condens. Matter Mater. Phys. 54 (23) (1996) 16533–16539.
[58] P. Hohenberg, W. Kohn, Inhomogeneous electron gas, Phys Rev. 136 (3B) (1964) B864–B871.
[59] M. Dolg, U. Wedig, H. Stoll, H. Preuss, Energy-adjusted ab initio pseudopotentials for the first row transition elements, J. Chem. Phys. 86 (2) (1987) 866–872.
[60] T.A. Halgren, W.N. Lipscomb, The synchronous-transit method for determining reaction pathways and locating molecular transition states, Chem. Phys. Lett. 49 (2) (1977) 225–232.
[61] H. Orita, T. Kubo, T. Matsushima, A. Kokalj, DFT calculations of adsorption and decomposition of N_2O on Rh(100), J. Phys. Chem. C 114 (2010) 21444–21449.
[62] R.G. Zhang, J.R. Li, B.J. Wang, L.X. Ling, Fundamental studies about the interaction of water with perfect, oxygen-vacancy and pre-covered oxygen $Cu_2O(111)$ surfaces: thermochemistry, barrier, product, Appl. Sur. Sci. 279 (2013) 260–271.
[63] G. Henkelman, H. Jónsson, Improved tangent estimate in the nudged elastic band method for finding energy paths and saddle points, J. Chem. Phys. 113 (22) (2000) 9978–9985.
[64] B. Delley, Form molecules to solids with the Dmol3 approach, J. Chem. Phys. 113 (18) (2000) 7756–7764.
[65] B. Delley, An all-electron numerical method for solving the local density functional for polyatomic molecules, J. Chem. Phys. 92 (1) (1990) 508–517.
[66] W.J. Xiang, J. Liu, M. Chang, C.G. Zheng, The adsorption mechanism of elemental mercury on CuO(110) surface, Chem. Eng. J. 200–202 (2012) 91–96.
[67] G. Kim, X.X. Li, P. Blowers, Adsorption energies of mercury-containing species on CaO and temperature effects on equilibrium constants predicted by density functional theory calculation, Langmuir 25 (2009) 2781–2789.
[68] P. Blowers, G. Kim, The adsorption of mercury-species on relaxed and rumpled CaO(001) surfaces investigated by density functional theory, J. Mol. Model. 17 (2011) 505–514.
[69] E. Sasmaz, S. Aboud, J. Wilcox, Hg binding on Pd binary alloys and overlays, J. Phys. Chem. C 113 (2009) 7813–7820.
[70] S. He, J.S. Zhou, Y.Q. Zhu, Z.Y. Luo, M.J. Ni, K.F. Cen, Mercury oxidation over a vanadia-based selective catalytic reduction catalyst, Energy Fuels 23 (1) (2009) 253–259.
[71] C.L. Senior, A.F. Sarofim, T.F. Zeng, J.J. Helble, R. Mamani-Paco, Gas-phase transformations of mercury in coal-fired power plants, Fuel Process. Technol. 63 (1–2) (2000) 197–213.
[72] C.L. Senior, J.J. Helble, A.F. Sarofim, Emissions of mercury, trace elements, and fine particles from stationary combustion sources, Fuel Process. Technol. 65–66 (2000) 263–288.
[73] B.K. Gullett, B. Ghorishi, R. Keeney, F.E. Huggins, Mercuric chloride capture by alkaline sorbents, in: Proceeding of the Air and Waste Management Association 93rd Annual Meeting and Exhibition, Salt Lake City, UT, June 18–22, 2000. p. 259.
[74] D.H. Lim, J. Wilcox, Heterogeneous mercury oxidation on Au(111) from first principles, Environ. Sci. Technol. 47 (15) (2013) 8515–8522.
[75] M.W.M. Hisham, S.W. Bneson, Thermochemistry of the deacon process, J. Phys. Chem. 99 (16) (1995) 6194–6198.